iJRASET
International Journal For Research in Applied Science and Engineering Technology

# INTERNATIONAL JOURNAL FOR RESEARCH

IN APPLIED SCIENCE & ENGINEERING TECHNOLOGY

**Volume:** 9 **Issue:** XI **Month of publication:** November 2021

**DOI:** https://doi.org/10.22214/ijraset.2021.38988

www.ijraset.com

Call: 08813907089 | E-mail ID: ijraset@gmail.com

International Journal for Research in Applied Science & Engineering Technology (IJRASET)
*ISSN: 2321-9653; IC Value: 45.98; SJ Impact Factor: 7.429*
*Volume 9 Issue XI Nov 2021- Available at www.ijraset.com*

# Closed-Loop Control of a New High Step-Up Multi-Input Multi-Output DC-DC Converter

Dr. T. Murali Mohan[1], Manohari. K[2]
[1, 2]*Department of EEE, JNTUK, Kakinada, Andhra Pradesh, India*

***Abstract:*** ***A new multi-input multi-output dc-dc converter with high step-up capability for wide power ranges is proposed in this paper. The converter's number of inputs and outputs is arbitrary and independent of each other. The proposed topology combines the benefits of DC-DC boost and switched-capacitor converters. The number of input, output, and voltage multiplier stages is arbitrary and depends on the design conditions. First, the various operating modes of the proposed converter are discussed. The closed-loop control system also must be designed using state space representation and small-signal modelling. Finally, the operation of the proposed converter is derived from the simulation results.***

***Keywords: High power converter, Low voltage stress, Multi-Input Multi-Output (MIMO) converter, Non-isolated high step-up dc-dc converter, closed loop control.***

## I. INTRODUCTION

Most of the electrical systems are supplied by one type of energy source e.g. utility line power, the solar, wind, etc. in some cases some are powered by two sources like UPS (Uninterruptible power supplies). In the future, most of the systems will need interfacing of different energy sources, the interfacing of multiple sources results in improved reliability, flexibility, and utilization of preferred energy sources [1]. Using multiple inputs increases the reliability and utilization of renewable sources as most renewable energy sources have their outputs are in the form of DC voltage and the input source has its voltage and output characteristics e.g. Photovoltaic cells, fuel cells, etc.[2]. Therefore a multiple-input DC-DC Converter is used and similarly different loads operate on different voltages thus multiple outputs are required. This decides the requirement of a MIMO DC-DC Converter is needed.

By adopting multi-input multi-output DC-DC converters which reduce the cost, energy loss, and complexity of dc distribution systems. Because many home appliances are supplied by dc and various loads are often require different voltage levels. MIMO converters have not received as much attention as MISO or SIMO converters. MIMO converter has both advantages of MISO and SIMO topologies and provides more cost-effective solutions.

Recently, multi-input multi-output DC-DC converters are utilized to generate output voltages with various levels by combining the different input sources with various voltage-current characteristics in a single stage. Some MIMO converters are presented in future energy efficient homes [3], low power applications [4-6] and high voltage level application [7] and EV applications [8].

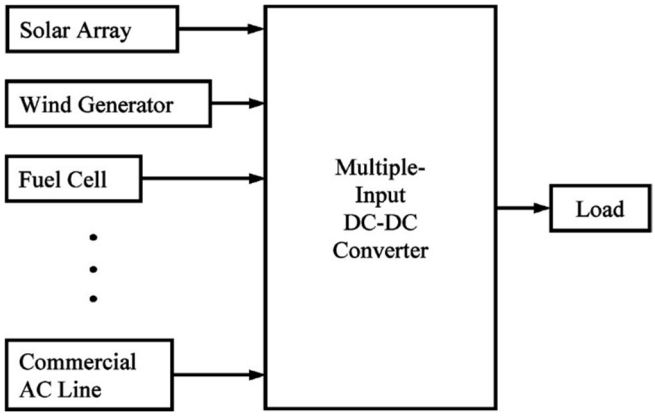


Figure.1. Block diagram of MIMO converter

As in DC systems, there are different types of loads that require different voltages and currents to run, so by obtaining different outputs from a single converter, they can be run successfully. The design is pretty simple, but there is a need to select an output and find its duty cycle of power switch. The greater the output voltage, the lesser the duty cycle. Whereas, select the duty cycle and find its output voltage.

In this paper, a new MIMO DC-DC converter with high output voltage levels is proposed. The proposed converter can continue its operation when one or some number of input sources have a fault or they are not able to provide the power of the output loads. In this case, the remaining other input sources can provide the power to the load. Also, the input faults will not affect the irrelevant outputs. It makes sure that the converter can continue its operation even with the failure of one or more capacitors at each output, providing the corresponding output power. Therefore, the proposed converter can be used in low or high power ranges with high efficiency.

## II. PROPOSED CONVERTER STRUCTURE AND OPERATIONAL PRINCIPLES

The structure of the proposed MIMO converter is shown in figure.1. In the proposed structure, for four input voltage sources, four inductors and four power switches are used. This makes the number of used power switches is minimum. The presented structure is composed of a number of diode-capacitor voltage multiplier stages. As shown in figure.1, all the inputs are based on the conventional boost converter. The Diode-Capacitor VM stages are alternately charged via their input cell which causes their corresponding output voltages to be increased. Each of the VM stages is composed of one capacitor and one diode and are denoted $C_{i,j,k}$ and $D_{i,j,k}$ respectively. i, j and k are the number of voltage multiplier stage, capacitor charger input number, corresponding output number of voltage multiplier, respectively.

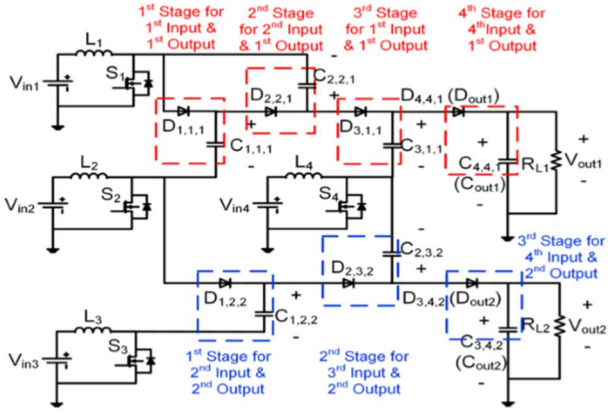


Figure.2. Four-input-two-output Boost converter

A four-input two-output proposed converter as shown in figure.2. For the first output, four stages of Diode-Capacitor VM (two stages for the first input, one stage for the second input, and one stage for the fourth input) are used. Also, for the second output, three stages of Diode-Capacitor VM (one stage for the second input, one stage for the third input, and one stage for the fourth input) are used. In the proposed converter, for normal operating condition of the converter, during turn-on, there should be an overlapping time between corresponding switches. Also, during a period of switching, at least one of the group corresponding power switches for each output must be turned off. Therefore, for each output, there is a 180-degree phase shift between the corresponding switches of the voltage multiplier even stages and odd stages. The duty cycle of the entire power switch must be greater than 50%. The switching signals of proposed four-input two-output is demonstrated in figure.3.

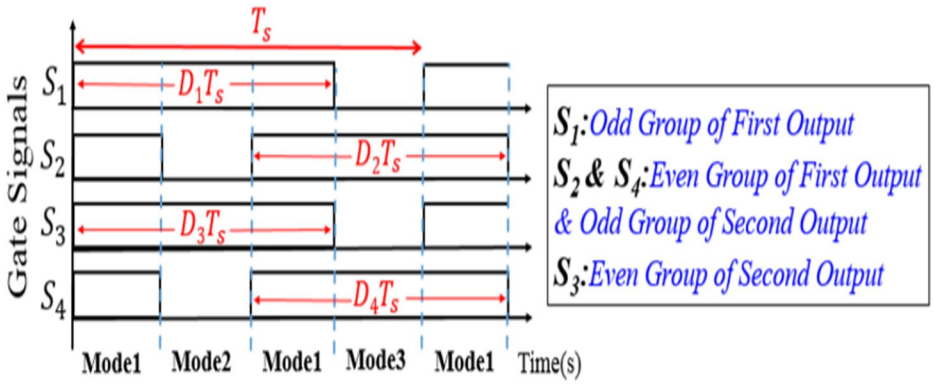


Figure.3. switching signals of proposed converter

*ISSN: 2321-9653; IC Value: 45.98; SJ Impact Factor: 7.429*
*Volume 9 Issue XI Nov 2021- Available at www.ijraset.com*

## III. OPERATION MODES

The operation of the proposed converter is analysed in continuous conduction mode by applying the same duty cycle for each and every switch. The proposed converter has three modes of operation, which are shown in the figure. 4.

### *A. First Mode of Operation*

As shown in figure.4 (a), in this mode all the four power switches are in ON state and all the inductors are magnetised through their input voltages and their currents are increased linearly. All the diodes are reverse biased and the VM capacitors do not charge or discharge and have constant voltage, except the capacitor of the last multiplier stage of each output. Moreover, the first and second output voltages are supplied through the last VM stage capacitors $C_{4.4,1}$ and $C_{3,4,2}$ respectively. The equations can be written as

$$V_{L_i-ON}=V_{in_i} \quad i = \{1,2,3,4\} \tag{1}$$

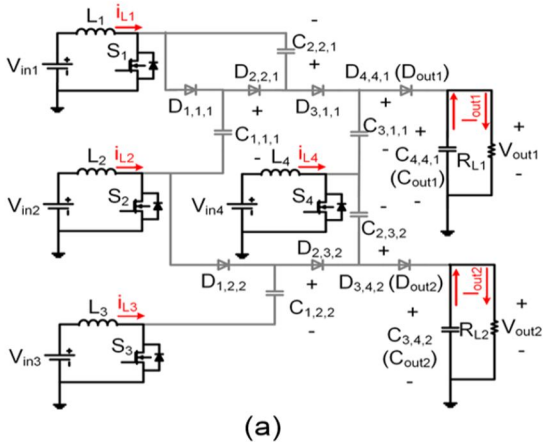


Figure.4(a). First mode of operation of four-input two-output Boost converter

### *B. Second Mode of Operation*

As shown in figure.4 (b), in this mode, only $S_1$and $S_3$ are in ON state and the current of inductors $L_1$and $L_3$ are increased linearly. The diodes of $D_{1,1,1}$ , $D_{3,1,1}$ and $D_{2,3,2}$ are reverse biased. And the diodes of $D_{2,2,1}$ , $D_{4,4,1}$, $D_{1,2,2}$ and $D_{3,4,2}$ are directly biased and conduct. The stored current of inductors $L_2$ and $L_4$ charges the capacitors $C_{2,2,1}$, $C_{4,4,1}$ of first output and capacitors $C_{1,2,2}$, $C_{3,4,2}$ of second output. The current of inductors $L_2$ and $L_4$ discharges the capacitors $C_{1,1,1}$ , $C_{3,1,1}$ of first output and capacitors $C_{2,3,2}$ of second output.

The load of two outputs is supplied via the stored current in the inductor $L_4$ of last input cell. The following equations are obtained.

$$V_{L_i-ON} = V_{in_i} \ , i = \{1,3\} \tag{2}$$

$$V_{L2-OFF} = V_{in_2} + V_{C_{1,1,1}} - V_{C_{2,2,1}} = V_{in_2} - V_{C_{1,2,2}} \tag{3}$$

$$V_{L4-OFF} = V_{in_4} + V_{C_{3,1,1}} - V_{C_{4,4,1}} = V_{in_4} + V_{C_{3,1,1}} - V_{out1}$$
$$= V_{in_4} + V_{C_{2,3,2}} - V_{C_{3,4,2}} = V_{in_4} + V_{C_{2,3,2}} - V_{out2} \tag{4}$$

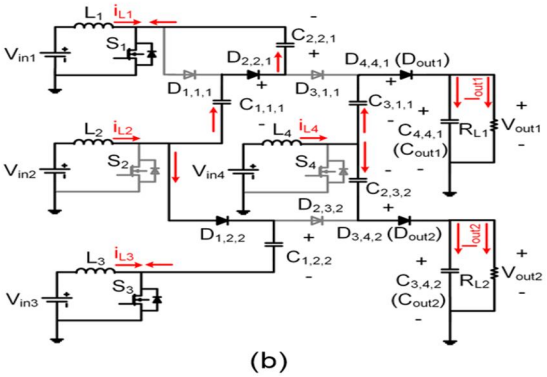


Figure.4(b). Second mode of operation of four-input two-output Boost converter

*C. Third Mode of Operation*

As shown in figure.4(c) in this mode, only $S_2$and $S_4$ are in ON state and the current of inductors $L_2$and $L_4$ are increased linearly. The diodes of $D_{2,2,1}$, $D_{4,4,1}$, $D_{1,2,2}$ and $D_{3,4,2}$ are reverse biased. And the diodes of $D_{1,1,1}$, $D_{3,1,1}$ and $D_{2,3,2}$ are directly biased and conduct. The stored current of inductors $L_1$ and $L_3$ charges the capacitors capacitors $C_{1,1,1}$, $C_{3,1,1}$ of first output and capacitors $C_{2,3,2}$ of second output. The stored current of inductors $L_2$ and $L_4$ discharges the capacitors $C_{2,2,1}$, $C_{4,4,1}$ of first output and capacitors $C_{1,2,2}$, $C_{3,4,2}$ of second output. The load of two outputs is supplied via the capacitor of last VM stage $C_{4,4,1}$ and $C_{3,4,2}$. The following equations are obtained.

$$V_{L_i-ON} = V_{in_i}, i = \{2,4\} \quad (5)$$

$$V_{L1-OFF} = V_{in_1} - V_{C_{1,1,1}} = V_{in_1} + V_{C_{2,2,1}} - V_{3,1,1} \quad (6)$$

$$V_{L3-OFF} = V_{in_3} + V_{C_{1,2,2}} - V_{C_{2,3,2}} \quad (7)$$

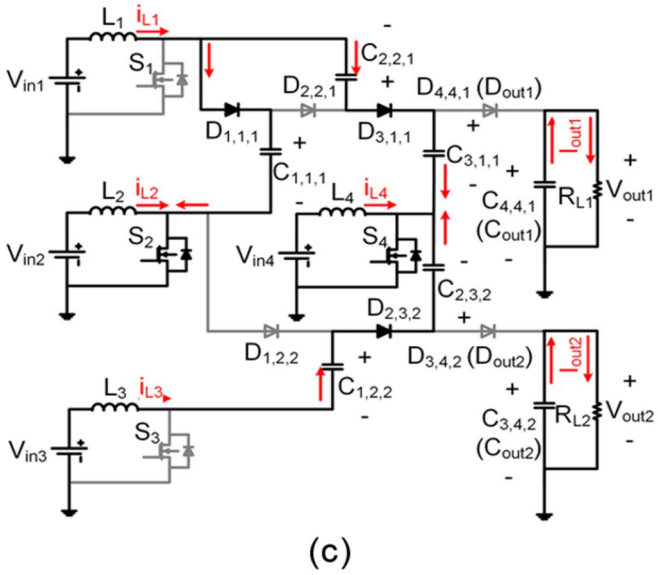


(c)

Figure.4(c). Third mode of operation of four-input two-output Boost converter

In order to calculate the output voltages and the voltage of capacitors, the volt-second balance law is used for entire input inductors. By using this law from equation (1)-(7), the capacitor voltages are obtained as

$$V_{C_{1,1,1}} = \frac{1}{1-D_1} V_{in_1} \quad (8)$$

$$V_{C_{2,2,1}} = \frac{1}{1-D_1} V_{in_1} + \frac{1}{1-D_2} V_{in_2} \quad (9)$$

$$V_{C_{3,1,1}} = \frac{2}{1-D_1} V_{in_1} + \frac{1}{1-D_2} V_{in_2} \quad (10)$$

$$V_{out1} = V_{C_{4,4,1}} = \frac{2}{1-D_1} V_{in_1} + \frac{1}{1-D_2} V_{in_2} + \frac{1}{1-D_4} V_{in_4} \quad (11)$$

$$V_{C_{1,2,2}} = \frac{1}{1-D_2} V_{in_2} \quad (12)$$

$$V_{C_{2,3,2}} = \frac{1}{1-D_2} V_{in_2} + \frac{1}{1-D_3} V_{in_3} \quad (13)$$

$$V_{out2} = V_{C_{3,4,2}} = \frac{1}{1-D_2} V_{in_2} + \frac{1}{1-D_3} V_{in_3} + \frac{1}{1-D_4} V_{in_4} \quad (14)$$

From (8)-(14), $D_1$, $D_2$, $D_3$ and $D_4$ are the duty cycles of switches $S_1$, $S_2$, $S_3$ and $S_4$ respectively.

*ISSN: 2321-9653; IC Value: 45.98; SJ Impact Factor: 7.429*
*Volume 9 Issue XI Nov 2021- Available at www.ijraset.com*

## IV. DESIGN OF COMPONENTS

### A. *Inductors Design*

The value of the inductor is designed for the converter to operate in continuous conduction mode. To calculate the size of the inductors, the inductor average current and ripple current must be calculated.

$$I_{L1_{avg}} = \frac{1}{1-D_1} I_{out1} \quad (15)$$

$$I_{L2_{avg}} = \frac{I_{out1}+I_{out2}}{1-D_2} \quad (16)$$

$$I_{L3_{avg}} = \frac{I_{out2}}{1-D_3} \quad (17)$$

$$I_{L4_{avg}} = \frac{I_{out1}+I_{out2}}{1-D_4} \quad (18)$$

The current ripple for each of the inductors is determined as

$$\Delta I_{Li} = \frac{D_i V_{in_i}}{L_i f_s}, \quad i = \{1,2,3,4\} \quad (19)$$

$\Delta I_{Li}$ and $f_s$ are the inductor current ripple and switching frequency respectively. using (15-18) and (19) the minimum value of inductors is calculated.

$$L_1 \geq \frac{D_1(1-D_1)V_{in1}}{2f_s I_{out1}} \quad (20)$$

$$L_2 \geq \frac{D_2(1-D_2)V_{in2}}{2f_s(I_{out1}+I_{out2})} \quad (21)$$

$$L_3 \geq \frac{D_3(1-D_3)V_{in3}}{2f_s I_{out2}} \quad (22)$$

$$L_4 \geq \frac{D_4(1-D_4)V_{in2}}{2f_s(I_{out1}+I_{out2})} \quad (23)$$

Using (15-18) and (19) the maximum current value of the inductor can be written as follows

$$I_{Li,max} = I_{Li,avg} + \frac{D_i V_{ini}}{2L_i f_s} \quad i = \{1,2,3,4\} \quad (24)$$

### B. *Capacitors Design*

The capacitor of last voltage multiplier stage for two outputs is chosen based on the transferred charge to the outputs to provide the desired voltage ripple of the each of the outputs. The capacitance value of the output capacitor for *k*th output is equal to

$$C_{out_k} = C_{i,j,k} = \frac{I_{out_k}}{f_s \Delta V_{out_k}} D_j, \quad i,j,k = \{1,2,3\ldots\} \quad (25)$$

Also, the value of the other capacitors for *k*th output is equal to

$$C_{i,j,k} = \frac{I_{out_k}}{f_s \Delta V_C}, \quad i,j,k = \{1,2,3\ldots\} \quad (26)$$

## V. STATE SPACE REPRESENTATION

The converter's dynamic characteristics are crucial for controller design and stability assessment. The state space and transfer function are two ways of representing the dynamic model of any converter, which is made up of linear circuit elements such as resistors, inductors, and capacitors, as well as non-linear circuit elements known as semiconductor switches. However, the resulting circuit for each switching operation is a linear circuit. As a result, developing a dynamic and output equation for each switching operation is feasible. Because the energy storage elements in the converter are dynamic, each element is linked to a dynamic variable.

Hence, the inductor current ($i_L$) and the capacitor voltage ($V_C$) are considered as the dynamic variables in this converter model. The small signal model concept is essential for developing an effective dynamic model for an optimised converter. After developing the small-signal equivalent circuit, the transfer function from any input to any output can be easily derived.
Therefore, the dynamic behaviour of this proposed converter can be described in a matrix form to perform its frequency domain based analysis based on the derived transfer functions.

The average model of the converter is given as follows:

*1) When Switches are ON (DT mode)*

$$\frac{di_{L_1}}{dt} = \frac{V_{in1}}{L_1} \quad (27)$$

$$\frac{di_{L_2}}{dt} = \frac{V_{in2}}{L_2} \quad (28)$$

$$\frac{di_{L_3}}{dt} = \frac{V_{in3}}{L_3} \quad (29)$$

$$\frac{di_{L_4}}{dt} = \frac{V_{in4}}{L_4} \quad (30)$$

$$\frac{dV_{C_{1,1,1}}}{dt} = \frac{-i_{L_2}}{C_{1,1,1}} \quad (31)$$

$$\frac{dV_{C_{1,2,2}}}{dt} = \frac{-i_{L_3}}{C_{1,1,1}} + \left(\frac{i_{L_1}+i_{L_2}+i_{L_3}-i_{L_4}}{2*C_{1,1,1}}\right) \quad (32)$$

$$\frac{dV_{C_{2,3,,2}}}{dt} = \left(\frac{-i_{L_1}-i_{L_2}-i_{L_4}}{C_{2,3,2}}\right) \quad (33)$$

$$\frac{dV_{C_{3,4,2}}}{dt} = \left(\frac{-i_{L_1}-i_{L_2}-i_{L_3}+i_{L_4}}{2*C_{3,4,2}}\right) \quad (34)$$

*2) When Switches are OFF ((1-D)T mode)*

$$\frac{di_{L_1}}{dt} = \frac{V_{in1}}{L_1} - \frac{V_{C1,1,1}}{L_1} \quad (35)$$

$$\frac{di_{L_2}}{dt} = \frac{V_{in2}}{L_2} - \frac{V_{C1,2,2}}{L_2} \quad (36)$$

$$\frac{di_{L_3}}{dt} = \frac{V_{in3}}{L_3} + \frac{V_{C1,2,2}}{L_3} - \frac{V_{C2,3,2}}{L_3} \quad (37)$$

$$\frac{di_{L_4}}{dt} = \frac{V_{in4}}{L_4} + \frac{V_{C2.3,2}}{L_4} - \frac{V_{C3,4,2}}{L_4} \quad (38)$$

$$\frac{dV_{C_{1,1,1}}}{dt} = \frac{-i_{L_2}}{C_{1,1,1}} \quad (39)$$

$$\frac{dV_{C_{1,2,2}}}{dt} = \frac{-i_{L_3}}{C_{1,1,1}} + \left(\frac{i_{L_1}+i_{L_2}+i_{L_3}-i_{L_4}}{2*C_{1,1,1}}\right) \quad (40)$$

$$\frac{dV_{C_{2,3,,2}}}{dt} = \left(\frac{-i_{L_1}-i_{L_2}-i_{L_4}}{C_{2,3,2}}\right) \quad (41)$$

$$\frac{dV_{C_{3,4,2}}}{dt} = \left(\frac{-i_{L_1}-i_{L_2}-i_{L_3}+i_{L_4}}{2*C_{3,4,2}}\right) \quad (42)$$

In the proposed MIMO converter, all the input voltages are fed by renewable energy sources, and the generating power depends on their environmental conditions. Therefore, a proper control method is required to draw maximum power from the input sources.

A small signal model is necessary to design the closed-loop control system. The state space model is used to reach the small signal model of the proposed MIMO converter.

$$\begin{cases} \dot{\tilde{x}} = A\tilde{x} + B\tilde{u} \\ \tilde{y} = C\tilde{x} \end{cases} \tag{43}$$

From the above equations, the state space model of the proposed converter can be expressed as,

$$A = \begin{bmatrix} 0 & 0 & 0 & 0 & \frac{-1}{L_1} & 0 & 0 & 0 \\ 0 & 0 & 0 & 0 & 0 & \frac{-1}{L_2} & 0 & 0 \\ 0 & 0 & 0 & 0 & 0 & \frac{1}{L_3} & \frac{-1}{L_3} & 0 \\ 0 & 0 & 0 & 0 & 0 & 0 & \frac{1}{L_4} & \frac{-1}{L_4} \\ 0 & \frac{-1}{C_{1,1,1}} & 0 & 0 & 0 & 0 & 0 & 0 \\ \frac{1}{2C_{1,2,2}} & \frac{1}{2C_{1,2,2}} & \frac{1}{C_{1,2,2}} & \frac{-1}{2C_{1,2,2}} & 0 & 0 & 0 & 0 \\ \frac{-1}{C_{2,3,2}} & \frac{-1}{C_{2,3,2}} & 0 & \frac{-1}{C_{2,3,2}} & 0 & 0 & 0 & 0 \\ \frac{-1}{2C_{3,4,2}} & \frac{-1}{2C_{3,4,2}} & \frac{-1}{2C_{3,4,2}} & \frac{1}{2C_{3,4,2}} & 0 & 0 & 0 & 0 \end{bmatrix} \tag{44}$$

$$B = \begin{bmatrix} \frac{V_1}{L_1} & 0 & 0 & 0 \\ 0 & \frac{V_2}{L_2} & 0 & 0 \\ 0 & 0 & \frac{V_3}{L_3} & 0 \\ 0 & 0 & 0 & \frac{V_4}{L_4} \\ 0 & 0 & 0 & 0 \\ 0 & 0 & 0 & 0 \\ 0 & 0 & 0 & 0 \\ 0 & 0 & 0 & 0 \end{bmatrix} \tag{45}$$

$$C = \begin{bmatrix} 0 & 0 & 0 & 0 & 1 & 0 & 0 & 0 \\ 0 & 0 & 0 & 0 & 0 & 1 & 0 & 0 \\ 0 & 0 & 0 & 0 & 0 & 0 & 1 & 0 \\ 0 & 0 & 0 & 0 & 0 & 0 & 0 & 1 \end{bmatrix} \tag{46}$$

$$D = \begin{bmatrix} 0 & 0 & 0 & 0 \\ 0 & 0 & 0 & 0 \\ 0 & 0 & 0 & 0 \\ 0 & 0 & 0 & 0 \end{bmatrix} \tag{47}$$

$$\dot{\tilde{x}} = \begin{bmatrix} \tilde{\imath}_{L_1} \\ \tilde{\imath}_{L_2} \\ \tilde{\imath}_{L_3} \\ \tilde{\imath}_{L_4} \\ \tilde{v}_{C_{1,1,1}} \\ \tilde{v}_{C_{1,2,2}} \\ \tilde{v}_{C_{2,3,2}} \\ \tilde{v}_{C_{out2}} \end{bmatrix} \quad \tilde{u} = \begin{bmatrix} \tilde{d}_1 \\ \tilde{d}_2 \\ \tilde{d}_3 \\ \tilde{d}_4 \end{bmatrix} \quad \tilde{y} = \begin{bmatrix} \tilde{\imath}_{L_1} \\ \tilde{\imath}_{L_2} \\ \tilde{\imath}_{L_3} \\ \tilde{\imath}_{L_4} \end{bmatrix} \tag{48}$$

Where, $\tilde{x}, \tilde{u}$ and $\tilde{y}$ are state variables vector, control variables vector, and system outputs vector, respectively.

A is the state matrix, B is the input matrix, C is the output matrix, and D is the feed-forward matrix. The converter control system is aimed to regulate the state variables $\tilde{\imath}_{L_1}$, $\tilde{\imath}_{L_2}$ , $\tilde{\imath}_{L_3}$ , $\tilde{\imath}_{L_4}$ $\tilde{v}_{c_{1,1,1}}$, $\tilde{v}_{c_{1,2,2}}$, $\tilde{v}_{c_{2,3,2}}$, $\tilde{v}_{c_{out1}}$ through their corresponding controlling variables $\tilde{d}_1, \tilde{d}_2, \tilde{d}_3, \tilde{d}_4$ respectively.

Where $A(n \times n)$ fixed matrix, $B(n \times r)$ fixed matrix and $C(m \times n)$ fixed matrix they can be explained in Refs [9, 10 and 11] and $m, n$ and $r$ are the numbers of output variables, state variables and control signals, respectively.

$$\begin{bmatrix} \frac{d\tilde{\imath}_{L_1}}{dt} \\ \frac{d\tilde{\imath}_{L_2}}{dt} \\ \frac{d\tilde{\imath}_{L_3}}{dt} \\ \frac{d\tilde{\imath}_{L_4}}{dt} \\ \frac{d\tilde{v}_{C_{1,1,1}}}{dt} \\ \frac{d\tilde{v}_{C_{1,2,2}}}{dt} \\ \frac{d\tilde{v}_{C_{2,3,2}}}{dt} \\ \frac{d\tilde{v}_{out2}}{dt} \end{bmatrix} = \begin{bmatrix} 0 & 0 & 0 & 0 & \frac{-1}{L_1} & 0 & 0 & 0 \\ 0 & 0 & 0 & 0 & 0 & \frac{-1}{L_2} & 0 & 0 \\ 0 & 0 & 0 & 0 & 0 & \frac{1}{L_3} & \frac{-1}{L_3} & 0 \\ 0 & 0 & 0 & 0 & 0 & 0 & \frac{1}{L_4} & \frac{-1}{L_4} \\ 0 & \frac{-1}{C_{1,1,1}} & 0 & 0 & 0 & 0 & 0 & 0 \\ \frac{1}{2C_{1,2,2}} & \frac{1}{2C_{1,2,2}} & \frac{1}{C_{1,2,2}} & \frac{-1}{2C_{1,2,2}} & 0 & 0 & 0 & 0 \\ \frac{-1}{C_{2,3,2}} & \frac{-1}{C_{2,3,2}} & 0 & \frac{-1}{C_{2,3,2}} & 0 & 0 & 0 & 0 \\ \frac{-1}{2C_{3,4,2}} & \frac{-1}{2C_{3,4,2}} & \frac{-1}{2C_{3,4,2}} & \frac{1}{2C_{3,4,2}} & 0 & 0 & 0 & 0 \end{bmatrix} \begin{bmatrix} \tilde{\imath}_{L_1} \\ \tilde{\imath}_{L_2} \\ \tilde{\imath}_{L_3} \\ \tilde{\imath}_{L_4} \\ \tilde{v}_{C_{1,1,1}} \\ \tilde{v}_{C_{1,2,2}} \\ \tilde{v}_{C_{2,3,2}} \\ \tilde{v}_{C_{out2}} \end{bmatrix} + \begin{bmatrix} \frac{V_1}{L_1} & 0 & 0 & 0 \\ 0 & \frac{V_2}{L_2} & 0 & 0 \\ 0 & 0 & \frac{V_3}{L_3} & 0 \\ 0 & 0 & 0 & \frac{V_4}{L_4} \\ 0 & 0 & 0 & 0 \\ 0 & 0 & 0 & 0 \\ 0 & 0 & 0 & 0 \\ 0 & 0 & 0 & 0 \end{bmatrix} \begin{bmatrix} \tilde{d}_1 \\ \tilde{d}_2 \\ \tilde{d}_3 \\ \tilde{d}_4 \end{bmatrix} \quad (49)$$

$$\begin{bmatrix} \tilde{\imath}_{L_1} \\ \tilde{\imath}_{L_2} \\ \tilde{\imath}_{L_3} \\ \tilde{\imath}_{L_4} \end{bmatrix} = \begin{bmatrix} 0 & 0 & 0 & 0 & 1 & 0 & 0 & 0 \\ 0 & 0 & 0 & 0 & 0 & 1 & 0 & 0 \\ 0 & 0 & 0 & 0 & 0 & 0 & 1 & 0 \\ 0 & 0 & 0 & 0 & 0 & 0 & 0 & 1 \end{bmatrix} \begin{bmatrix} \tilde{\imath}_{L_1} \\ \tilde{\imath}_{L_2} \\ \tilde{\imath}_{L_3} \\ \tilde{\imath}_{L_4} \\ \tilde{v}_{C_{1,1,1}} \\ \tilde{v}_{C_{1,2,2}} \\ \tilde{v}_{C_{2,3,2}} \\ \tilde{v}_{C_{out2}} \end{bmatrix} \quad (50)$$

## VI. POLE PLACEMENT METHOD via INTEGRAL STATE FEEDBACK

The proposed MIMO converter has to be controlled by pole placement method (via integral state feedback) to reach a suitable control method [13]. This control method is shown in fig.5.

The location of the desired closed-loops is required for proper design of the state feedback gain matrix. This can be written with equation (43)

$$\begin{cases} \tilde{u} = -K_x\tilde{x} - K_q q \\ q = r - \tilde{y}^{\cdot} = r - C'\tilde{x} \end{cases} \quad (53)$$

Where $q$ is the integrator output and $r$ is the reference signals vector for the output variables of the proposed converter. The MIMO control system is complete states controllable. The controllability matrix of this system is defined as

$$\emptyset_c = [B|AB|A^2B| \dots |A^{n-1}B] \quad (54)$$

If the rank of the controllability matrix $\emptyset_c$ is complete $rank\ (\emptyset_c) = n$, then the system is complete state controllable.

By combining the equations (43) and (49) the new state space model for the converter is as follows

$$\begin{bmatrix} \dot{\tilde{x}}(t) \\ \dot{q}(t) \end{bmatrix} = \overbrace{\begin{bmatrix} A & 0 \\ -C & 0 \end{bmatrix}}^{\hat{A}} \begin{bmatrix} \tilde{x}(t) \\ q(t) \end{bmatrix} + \overbrace{\begin{bmatrix} B \\ 0 \end{bmatrix}}^{\hat{B}} \tilde{u}(t) + \begin{bmatrix} 0 \\ I \end{bmatrix} r(t) \quad (55)$$

$$\tilde{y}(t) = [C \quad 0] \begin{bmatrix} \tilde{x}(t) \\ q(t) \end{bmatrix} \quad (56)$$

The obtained system should be complete state controllable. If the following matrix $rank\ is\ n + m$, the defined system is complete state controllable.

$$M = \begin{bmatrix} B & A \\ 0 & -C \end{bmatrix}; rank(M) = n + m \quad (57)$$

Equation (53) guarantees that there is a feedback matrix $K = [K_x \quad K_q]$, which places closed-loop poles in arbitrary places. This state feedback can be entered into the control system as

$$\tilde{u}(t) = -K \begin{bmatrix} \tilde{x}(t) \\ q(t) \end{bmatrix} = -[K_x \quad K_q] \begin{bmatrix} \tilde{x}(t) \\ q(t) \end{bmatrix} \quad (58)$$

By importing (54) in (51 and 52) the state equations of the control system as follows:

$$\begin{bmatrix} \dot{\tilde{x}}(t) \\ \dot{q}(t) \end{bmatrix} = \begin{bmatrix} A - BK_x & -BK_q \\ -C & 0 \end{bmatrix} \begin{bmatrix} \tilde{x}(t) \\ q(t) \end{bmatrix} + \begin{bmatrix} 0 \\ I \end{bmatrix} r(t) \quad (59)$$

By specifying the desired closed loop poles of $\hat{A}' - \hat{B}'K$ as $\mu_1, \mu_2, \ldots . \mu_{(n+m)}$ the state feedback gain matrix $K_x$ and integral gain constant $K_q$ can be determined by the control system toolbox of the MATLAB software.

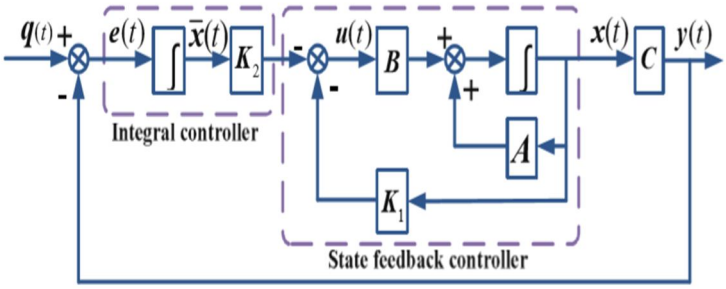


Figure.5.Closed loop control system schematic diagram of four-input two-output Boost converter

After determining the system state feedback matrixes $K_x$ and $K_q$, several different possible operating points are defined for the converter output voltages. Afterwards for each operating point, converter small signal model and its eigenvalues are obtained from matrix $\hat{A}$. For each case, the nearest real part of the Eigen values to the $j\omega$ axis shows the converter stability margin in the operating point.

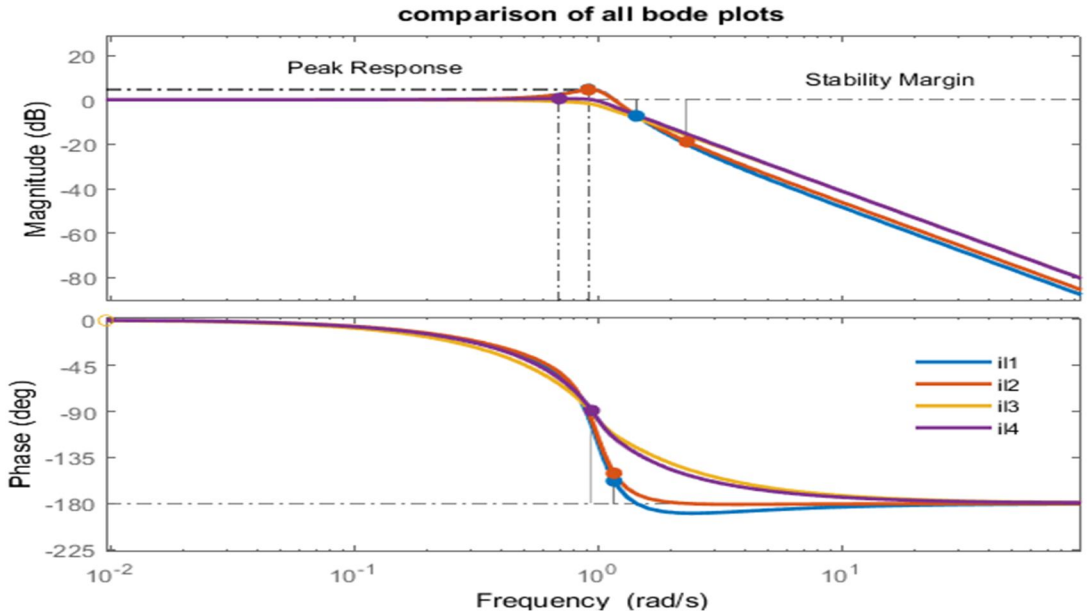


Figure12: Bode plots for the transfer functions of the inductor currents

The bode-plots of the four-input-two-input converter system after controllers as shown in figure. A Bode Plot is a useful tool that shows the gain and phase response of a given LTI system for different frequencies. The desired closed loop poles should be determined to reach the gain margin of GM≥10 and phase margin of 60°≤ PM≤ 90°.

The transfer function matrix of the converter is obtained from the small signal model [12]. The rank of transfer function matrix denotes the number of control variables. In this paper, according to the number of control variables and based on (48), rank of transfer function matrix G is 4×4.

$$\underbrace{\begin{bmatrix} y_1 \\ y_2 \\ y_3 \\ y_4 \end{bmatrix}}_{\hat{y}} = \underbrace{\begin{bmatrix} g_{11} & g_{12} & g_{13} & g_{14} \\ g_{21} & g_{22} & g_{23} & g_{24} \\ g_{31} & g_{32} & g_{33} & g_{34} \\ g_{41} & g_{42} & g_{34} & g_{44} \end{bmatrix}}_{\hat{G}} \underbrace{\begin{bmatrix} u_1 \\ u_2 \\ u_3 \\ u_4 \end{bmatrix}}_{\hat{u}} \tag{51}$$

There are the four transfer functions as follows:

$$\begin{cases} \frac{\hat{\imath}_{L_1}}{\hat{d}_1} = g_{11} = \frac{0.3813\ s^6 + 2.182\ s^5 + 5.549\ s^4 + 8.093\ s^3 + 7.3\ s^2 + 3.891\ s + 1}{s^8 + 5.126\ s^7 + 13.14\ s^6 + 21.85\ s^5 + 25.69\ s^4 + 21.85\ s^3 + 13.14\ s^2 + 5.126\ s + 1} \\ \frac{\hat{\imath}_{L_2}}{\hat{d}_2} = g_{22} = \frac{0.4918\ s^6 + 2.558\ s^5 + 6.121\ s^4 + 8.588\ s^3 + 7.548\ s^2 + 3.956\ s + 1}{s^8 + 5.126\ s^7 + 13.14\ s^6 + 21.85\ s^5 + 25.69\ s^4 + 21.85\ s^3 + 13.14\ s^2 + 5.126\ s + 1} \\ \frac{\hat{\imath}_{L_3}}{\hat{d}_3} = g_{33} = \frac{0.889\ s^6 + 3.35\ s^5 + 6.46\ s^4 + 8.036\ s^3 + 6.714\ s^2 + 3.636\ s + 1}{s^8 + 5.126\ s^7 + 13.14\ s^6 + 21.85\ s^5 + 25.69\ s^4 + 21.85\ s^3 + 13.14\ s^2 + 5.126\ s + 1} \\ \frac{\hat{\imath}_{L_4}}{\hat{d}_4} = g_{44} = \frac{0.8855\ s^6 + 3.591\ s^5 + 7.079\ s^4 + 8.81\ s^3 + 7.36\ s^2 + 3.895\ s + 1}{s^8 + 5.126\ s^7 + 13.14\ s^6 + 21.85\ s^5 + 25.69\ s^4 + 21.85\ s^3 + 13.14\ s^2 + 5.126\ s + 1} \end{cases} \tag{52}$$

Table 1
Components Characteristics

| Components | Values | Efficiency calculations |
|---|---|---|
| Output powers | $P_{out1}$=520W, $P_{out1}$=480W | 10W-5KW |
| Input voltages | $V_{in1}$=52V, $V_{in2}$=40V, $V_{in3}$=50V, $V_{in4}$=42V | $V_{in}$=50V |
| Switching frequency | 40KHz | 40KHz |
| Output voltages | $V_{out1}$=453V, $V_{out2}$=322V | $V_{out1}$=400V, $V_{out2}$=300V |
| Duty cycles | 0.6 | 0.5 |
| Inductors | $L_1$=$L_1$=$L_1$=$L_1$=400µH | $r_L$ = 80$m\Omega$ |
| Capacitors | 44µf,450V | $r_C$ = 20$m\Omega$ |
| Power switches | IRFP260 | $r_{DS}$ = 40$m\Omega$ |
| Power Diodes | STRP860DF | $r_D$ = 50$m\Omega$, $V_{FD}$ = 0.7$V$ |

Table 2
Tabular Form Of Output Voltages For Various Duty Cycles

| Duty cycle | $V_{out1}$(V) | $V_{out2}$(V) |
|---|---|---|
| 0.6 | 453.3 | 322.9 |
| 0.7 | 598.9 | 427.6 |
| 0.8 | 873.6 | 627.4 |
| 0.9 | 1526 | 1128 |
| 0.95 | 2033 | 1649 |

## VII. EFFICIENCY ANALYSIS

The efficiency of the proposed converter is presented with values of the components such as inductors equivalent resistance ($r_L$) and capacitors equivalent resistance ($r_C$), MOSFET ON-state resistance($r_{DS}$), Diodes forward resistance ($r_D$) and Diodes forward voltage($V_F$). For efficiency analysis of the converter, the current ripple of the inductors is neglected. Also the converter switching losses due to the major role in the converter efficiency are presented. Therefore, the RMS values of inductor currents are equal to average values.

$$I_{Lj-RMS} = I_{Lj-avg} \quad j = \{1,2,3,4\} \tag{60}$$

The conduction losses of the inductors $L_1, L_2, L_3$ and $L_4$ can be calculated as follows:

$$P_{r_{L1}} = r_{L1}\frac{4P_{out1}}{(1-D_1)^2 R_{Load1}} \tag{61}$$

$$P_{r_{L2}} = \frac{r_{L1}}{(1-D_2)^2}\left(\frac{P_{out1}}{R_{Load1}} + \frac{P_{out2}}{R_{Load2}} + \frac{2V_{out1}}{R_{Load1}}\frac{V_{out2}}{R_{Load2}}\right) \tag{62}$$

$$P_{r_{L3}} = r_{L3}\frac{P_{out2}}{(1-D_3)^2 R_{Load2}} \tag{63}$$

$$P_{r_{L4}} = \frac{r_{L4}}{(1-D_4)^2}\left(\frac{P_{out1}}{R_{Load1}} + \frac{P_{out2}}{R_{Load2}} + \frac{2V_{out1}}{R_{Load1}}\frac{V_{out2}}{R_{Load2}}\right) \tag{64}$$

Diode RMS current is written as follows:

$$I_{D_{i,j,k}-RMS} = \frac{I_{out_k}}{\sqrt{1-D_j}} \quad i,j = \{1,2,3,4\}, k = \{1,2\}$$

Therefore, the conduction losses of the diodes can be calculated as follows:

$$P_{r_{D_{i,j,k}}} = \frac{r_{D_{i,j,k}} P_{out_k}}{(1-D_j)R_{Load_k}} \quad i,j = \{1,2,3,4\}, k = \{1,2\}$$

The average current of diodes is essential for forwarding voltage losses of the diode. The forward losses of diodes can be calculated as follows:

$$P_{V_{F_{i,j,k}}} = \frac{V_{F_{i,j,k}} P_{out_k}}{V_{out_k}} \quad i,j = \{1,2,3,4\}, k = \{1,2\} \tag{65}$$

According to the operation modes, RMS currents of the VM capacitors are obtained as follows:

$$I_{C_{i,j,k}-RMS} = \sqrt{\frac{2-D_j-D_m}{(1-D_j)(1-D_m)} I_{out_k}} \quad i,j,m = \{1,2,3,4\}, \; k = \{1,2\}$$

$$I_{C_{out_k}-RMS} = \sqrt{\frac{D_4}{(1-D_4)} I_{out_k}} \quad k = \{1,2\} \tag{66}$$

Therefore, the conduction losses of capacitors are equal to:

$$P_{r_{C_{i,j,k}}} = r_{C_{i,j,k}}\frac{(2-D_j-D_m)P_{out_k}}{(1-D_j)(1-D_m)R_{Load_k}} \quad i,j,m = \{1,2,3,4\}, \; k = \{1,2\}$$

$$P_{r_{C_{i,j,k}}} = r_{C_{i,j,k}}\frac{D_4 P_{out_k}}{(1-D_4)R_{Load_k}} \quad k = \{1,2\} \tag{67}$$

Also, according to the operating modes of the converter, RMS currents of the power switches $S_1, S_2, S_3$ and $S_4$ are obtained as follows:

$$I_{S_1-RMS} = \sqrt{\frac{4I^2_{out1}}{(1-D_1)^2} + \frac{I^2_{out1}}{(1-D_2)}}$$

$$I_{S_2-RMS} = \sqrt{\frac{D_2 I^2_{out2} + (2-D_2) I^2_{out1} + 2I_{out1}I_{out2}}{(1-D_2)^2} + \frac{I^2_{out1}}{(1-D_1)}} \tag{68}$$

$$I_{S_3-RMS} = \sqrt{\frac{I^2_{out2}}{(1-D_3)^2} + \frac{I^2_{out_2}}{(1-D_2)}}$$

$$I_{S_4-RMS} = \sqrt{\frac{(2-D_4)(I_{out_1}+I_{out_2})^2}{(1-D_4)^2} + \frac{I_{out_1}(I_{out_2}+I_{out_1})}{(1-D_1)} + \frac{I^2_{out_2}}{(1-D_3)}}$$

So the conduction losses of the power switch $S_1, S_2, S_3$ and $S_4$ can be calculated as follows:

$$P_{r_{DS1}} = r_{DS1}\frac{4}{(1-D_1)^2} + \frac{1}{(1-D_2)}\frac{P_{out1}}{R_{Load1}}$$

$$P_{r_{DS2}} = r_{DS2}\frac{\frac{D_2P_{out2}}{R_{Load2}} + \frac{(2-D_2)P_{out1}}{R_{Load1}} + \frac{2V_{out1}V_{out2}}{R_{Load1}R_{Load2}}}{(1-D_2)^2} + \frac{P_{out1}}{(1-D_1)R_{Load1}}$$

$$P_{r_{DS3}} = r_{DS3}\frac{1}{(1-D_3)^2} + \frac{1}{(1-D_2)}\frac{P_{out2}}{R_{Load2}}$$

$$P_{r_{DS4}} = r_{DS4}\frac{(2-D_4)\left(\frac{P_{out1}}{R_{Load1}} + \frac{P_{out2}}{R_{Load2}} + \frac{2V_{out1}V_{out2}}{R_{Load1}R_{Load2}}\right)}{(1-D_4)^2} + \frac{\frac{P_{out1}}{R_{Load1}} + \frac{V_{out1}V_{out2}}{R_{Load1}R_{Load2}}}{(1-D_1)} + \frac{P_{out2}}{(1-D_3)R_{Load2}} \quad (69)$$

The switching losses of the proposed converter for the switches $S_1, S_2, S_3$ and $S_4$ can be calculated as follows:

$$P_{Sj-switching} = \frac{1}{2}I_{Lj}V_{Sj}\left(t_{ON_j} + t_{OFF_j}\right) + \frac{1}{2}f_sC_{Oj}V^2{}_{Sj} \quad j = \{1,2,3,4\} \quad (70)$$

In above equation, $C_{Oj}$ is the capacitor of each power switch or MOSFET. $f_S$,$V_{Sj}$ and $I_{Lj}$are the switching frequency, voltage across the power switch $S_j$ and the average current of inductor $L_j$ respectively. $t_{ON_j}$ and $t_{OFF_j}$ are the turn-on delay time and turn-off delay time of the power switch or MOSFET $S_j$. The efficiency of the four-input-two-output sample of the proposed converter can be calculated as follows:

$$\eta = \frac{P_{out-Total}}{P_{in-Total}} = \frac{P_{out1}+P_{out2}}{P_{out1}+P_{out2}+P_{Loss-Total}} \times 100\% \quad (71)$$

$$P_{Loss-Total} = P_{rL} + P_{rDS} + P_{rD} + P_{VF} + P_{rC} + P_{S-switching} \quad (72)$$

$$A_1 = \frac{P_{out1}}{R_{Load1}}, A_2 = \frac{P_{out2}}{R_{Load2}}$$

$$B_1 = \frac{V_{out1}}{R_{Load1}}, B_2 = \frac{V_{out2}}{R_{Load2}}$$

$$P_{r_{L1}} = r_{L1}\frac{4A_1}{(1-D_1)^2} + r_{L3}\frac{A_2}{(1-D_3)^2} + \left(\frac{r_{L2}}{(1-D_2)^2} + \frac{r_{L4}}{(1-D_4)^2}\right)(A_1 + A_2 + 2B_1B_2) \quad (73)$$

$$P_{r_{DS}} = r_{DS1}\left[\frac{4A_1}{(1-D_1)^2} + \frac{A_1}{(1-D_2)}\right] + r_{DS3}\left[\frac{A_2}{(1-D_3)^2} + \frac{A_2}{(1-D_2)}\right] + r_{DS2}\left[\frac{D_2A_2+(2-D_2)A_1+2B_1B_2}{(1-D_2)^2} + \frac{A_1}{(1-D_1)}\right] + r_{DS4}\left[\frac{(2-D_4)(A_1+A_2+2B_1B_2)}{(1-D_4)^2} + \frac{(2-D_2)(A_1+B_1B_2)}{(1-D_1)} + \frac{A_2}{(1-D_3)}\right] \quad (74)$$

$$P_{r_D} = r_{D1}\left[\frac{2A_1}{(1-D_1)} + \frac{A_1}{(1-D_2)} + \frac{A_1}{(1-D_4)}\right] + r_{D2}\left[\frac{A_2}{(1-D_2)} + \frac{A_2}{(1-D_3)} + \frac{A_2}{(1-D_4)}\right] \quad (75)$$

$$P_{r_C} = r_{C1}\left[\frac{2(2-D_1-D_2)A_1}{(1-D_1)(1-D_2)} + \frac{(2-D_1-D_4)A_1}{(1-D_1)(1-D_4)} + \frac{D_4A_1}{(1-D_4)}\right] + r_{C2}\left[\frac{(2-D_2-D_3)A_2}{(1-D_2)(1-D_3)} + \frac{(2-D_3-D_4)A_2}{(1-D_3)(1-D_4)} + \frac{D_4A_2}{(1-D_4)}\right] \quad (76)$$

$$P_{S-switching} = \sum_{j=1}^{4}\frac{1}{2}I_{Lj}V_{Sj}\left(t_{ON_j} + t_{OFF_j}\right) + \frac{1}{2}f_sC_{Oj}V^2{}_{Sj} \quad (77)$$

$$P_{VF} = 4V_{F1}B_1 + 3V_{F2}B_2 \quad (78)$$

Where $P_{rL}, P_{rDS}, P_{rD}, P_{VF}, P_{rC}$ and $P_{S-switching}$ are conduction losses of inductors, conduction losses of power switches, conduction losses of diodes, forward voltage losses of diodes, and switching losses of power switches.

*ISSN: 2321-9653; IC Value: 45.98; SJ Impact Factor: 7.429*
*Volume 9 Issue XI Nov 2021- Available at www.ijraset.com*

## VIII. SIMULATION AND RESULTS

The simulation diagram of a Four-input-two-output Boost converter is shown in figure.5. it can continue its operation when one or more input voltage sources have a fault and provide the required output voltage.

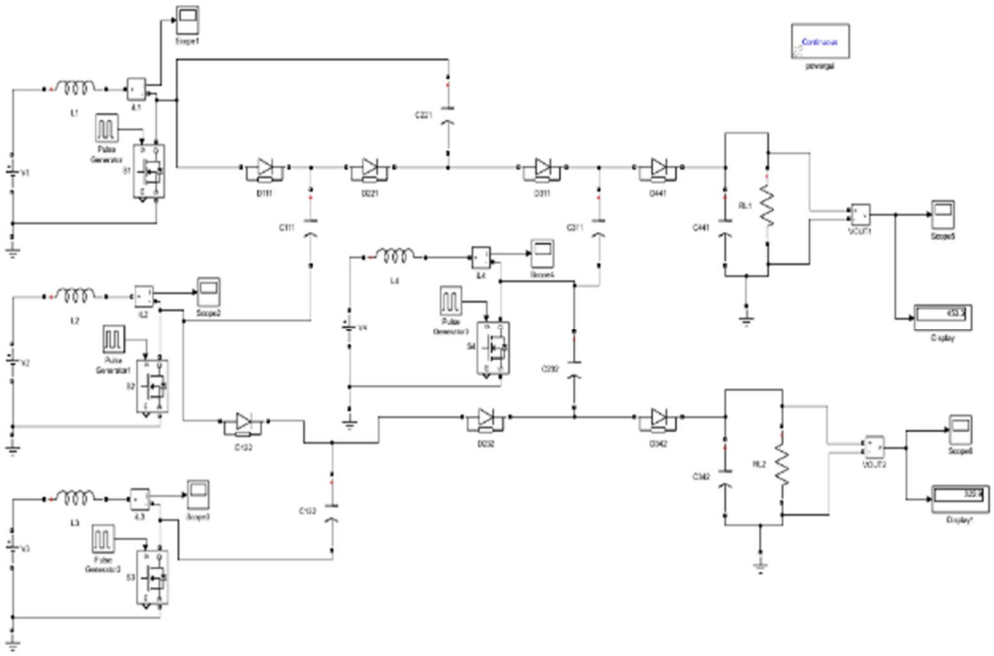

Figure.5. Simulation of a four-input two-output boost converter

Simulation has been done for the input voltage sources $V_{in1} = 52V$ , $V_{in2} = 40V$, $V_{in3} = 30V$ and $V_{in4} = 42V$ and the output voltage of the converter is desired to be regulated as $V_{out1} = 453V$and $V_{out2} = 322V$. The first output voltage $V_{out1}$=453V and second output voltage $V_{out2}$=322V which is shown in figure.6.

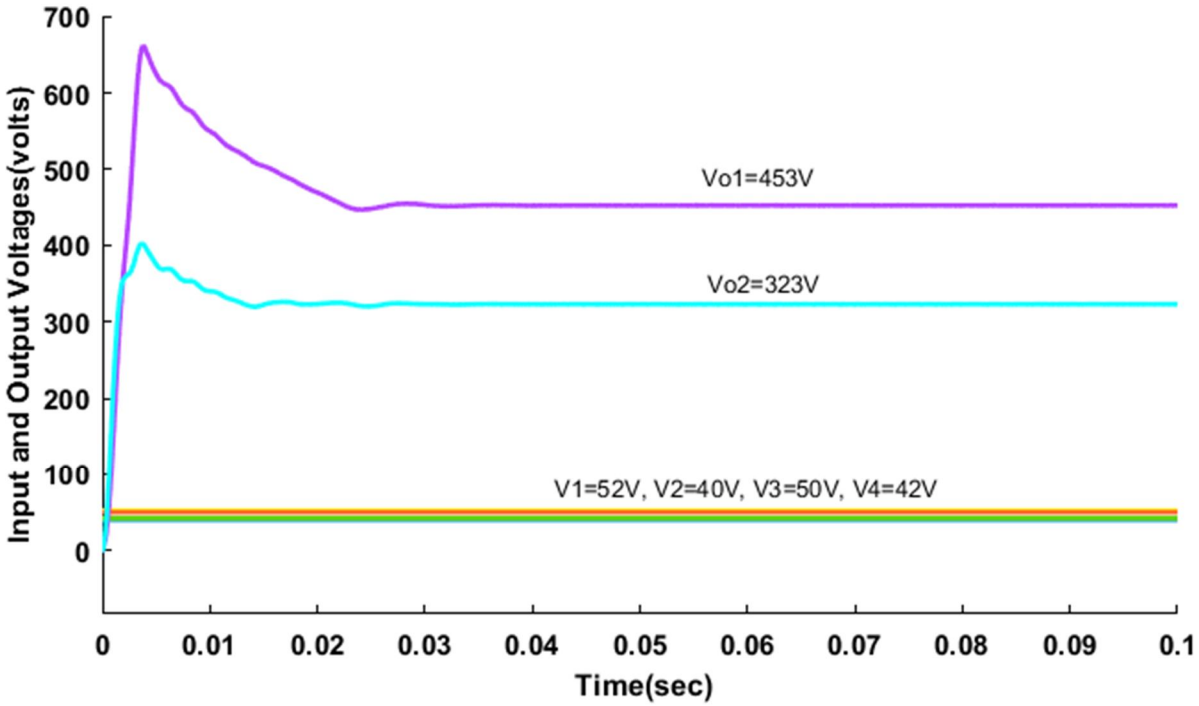


Figure.6. Input and Output voltages of four-input two-output boost converter

*ISSN: 2321-9653; IC Value: 45.98; SJ Impact Factor: 7.429*
*Volume 9 Issue XI Nov 2021- Available at www.ijraset.com*

Simulation has been done for the input voltage sources $V_{in1} = 52V$ , $V_{in2} = 40V$, $V_{in3} = 0V$ and $V_{in4} = 42V$ and the output voltage of the converter is desired to be regulated as $V_{out1} = 453V$and $V_{out2} = 200V$. The first output voltage $V_{out1}$=453V and second output voltage $V_{out2}$=200V which is shown in figure.7.

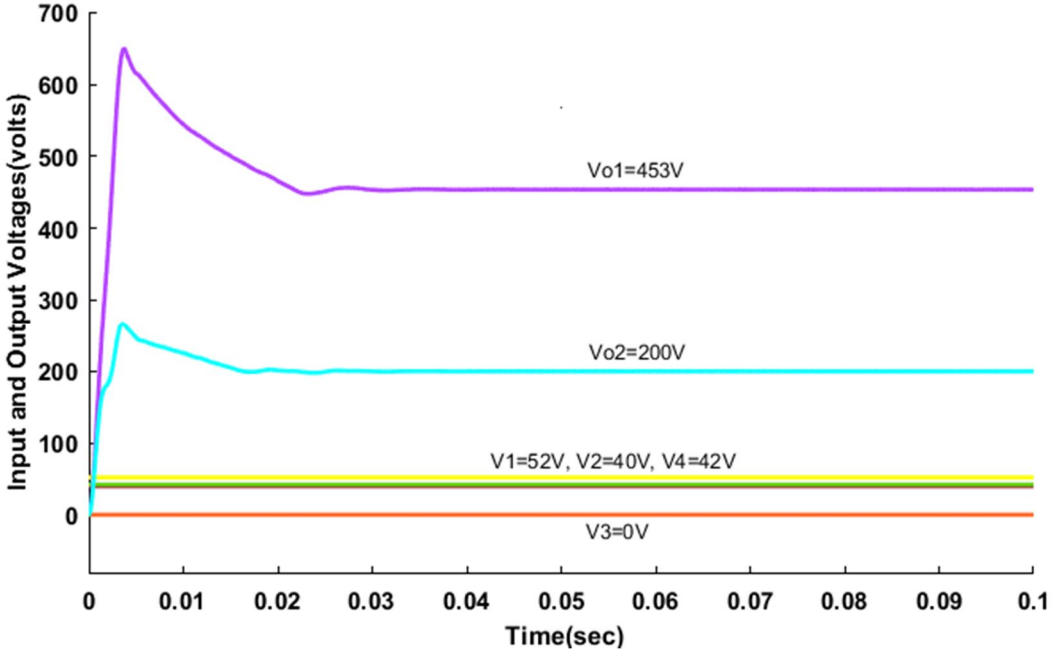


Figure.6. Input and Output voltages of four-input two-output boost converter

The waveforms of the inductors current $i_{L1}$ and $i_{L2}$ are shown in Figs. 7 and 8 respectively. The measured average current of inductors $L_1$ and $L_2$ is 7.07 A and 4.83 A. The calculated average current of inductors $L_1$ and $L_2$ is 7.59 A and 5.4 A. The measured current ripple of the inductors $L_1$ and $L_2$ are 2 A and 1.6 A, respectively.

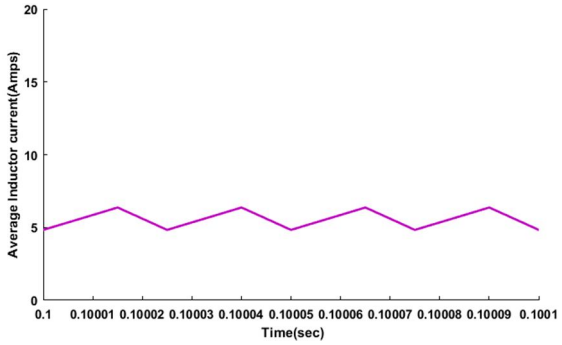


Figure.7.Average inductor current $i_{L_1}$ waveform

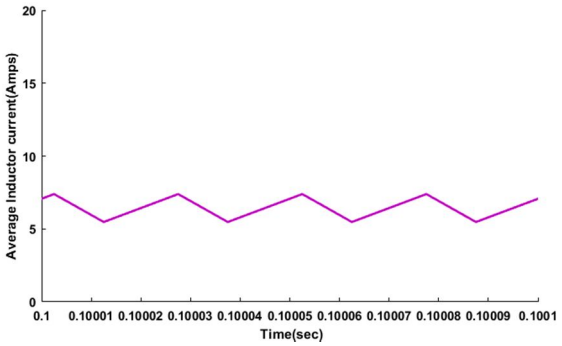


Figure.8. Average inductor current $i_{L_2}$ waveform

The waveforms of the inductors current $i_{L3}$ and $i_{L4}$ are shown in Figs. 5.16 and 5.17 respectively. The measured average current of inductors $L_3$ and $L_4$ is 3.19 A and 4.83 A .The calculated average current of inductors $L_3$ and $L_4$ is 3.54 A and 5.43 A. The measured current ripple of the inductors $L_3$ and $L_4$ are 2 A and 1.6 A, respectively.

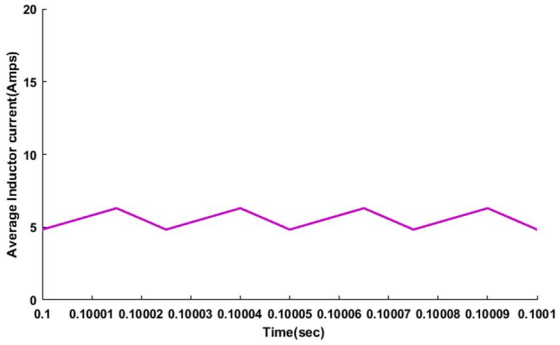


Figure.9. Average inductor current $i_{L_3}$ waveform

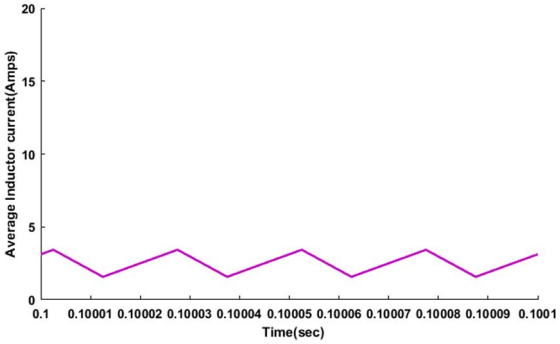


Figure.10. Average inductor current $i_{L_4}$ waveform

The maximum voltage stress across the power diodes are shown below. The voltage stress across the first VM diode of the first output $D_{1,1,1}$ and the first output diode $D_{out1}$ are obtained 225V and 100V respectively. The voltage stress across the first VM diode of the first output $D_{1,2,2}$ and $D_{2,3,2}$ are 218V and 224V respectively.

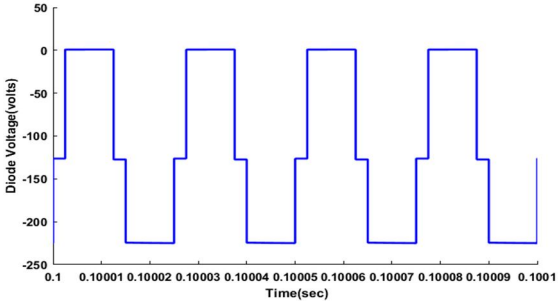


Figure.11(a). Diode $D_{1,1,1}$Voltage

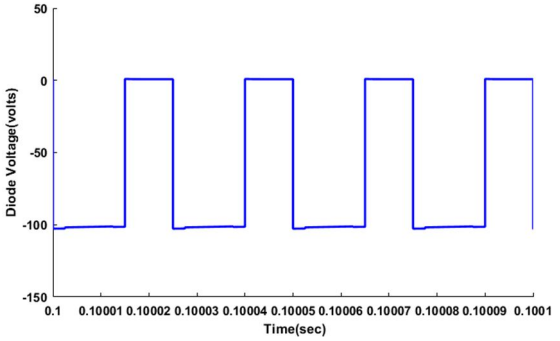


Figure.11(b). The first output diode $D_{out1}$Voltage

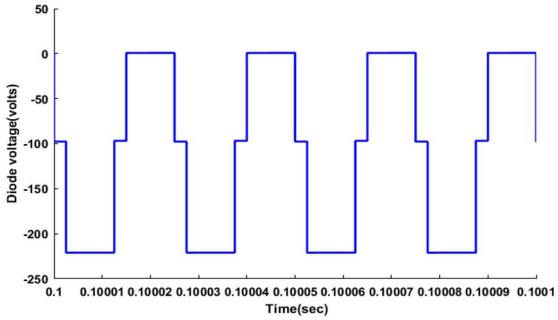


Figure.11(c). Diode $D_{1,2,2}$Voltage

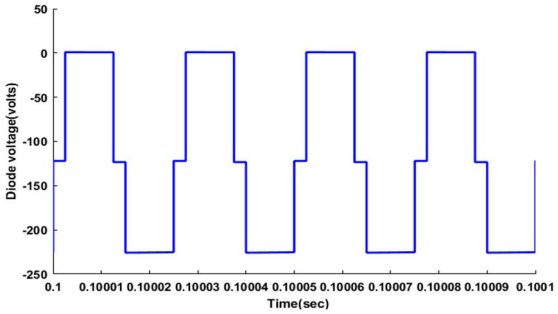


Figure.11(d). Diode $D_{2,3,2}$Voltage

The simulation diagram of a four-input-two-output Boost converter with PI controller is shown in figure.12. It can continue its operation when one or more input voltage sources have a fault and provide the required output voltage. Also switched capacitor is present in dc to dc converter circuit having four input voltage levels that can be converted to other voltage levels in boost mode, resulting in a wide range of output voltages. The duty cycle is adjusted with the help of a PI controller to achieve output voltage regulation in the dc-dc converter.

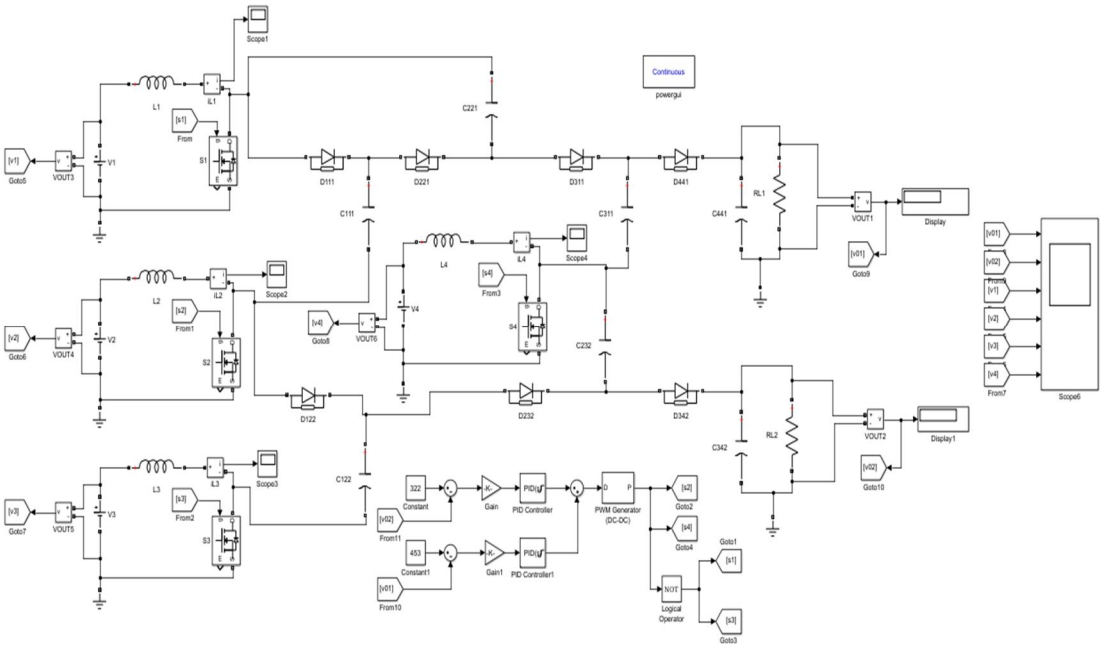


Figure.12. Simulation of a four-input-two-output Boost converter with PI controller

Simulation has been done for the input voltage sources $V_{in1} = 52V$ , $V_{in2} = 40V$, $V_{in3} = 0V$ and $V_{in4} = 42V$ and the output voltage of the converter is desired to be regulated as $V_{out1} = 465V$and $V_{out2} = 323V$.

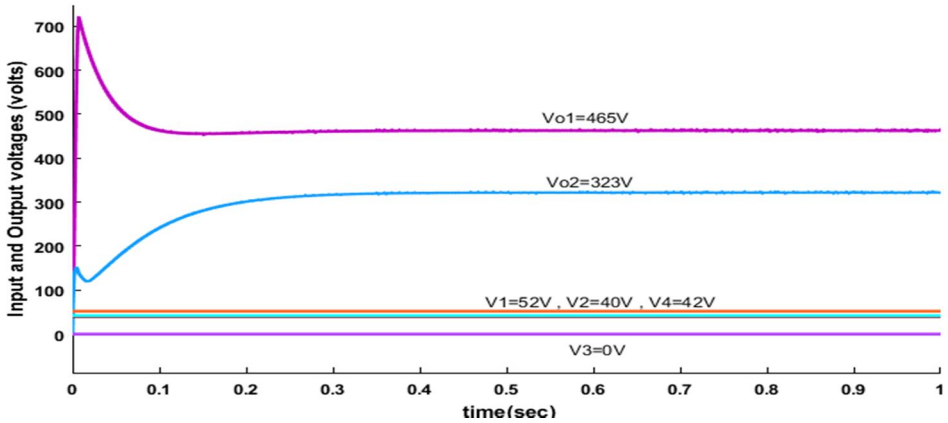


Figure.13.Input and Output Voltage waveforms of a four-input two-output Boost converter with PI controller

Even if the input is changed, the output must retain the desired value. As a result, the simulation for the input voltage sources $V_{in1} = 26V$ , $V_{in2} = 20V$, $V_{in3} = 25V$ and $V_{in4} = 21V$ and the output voltage of the converter is desired to be regulated as $V_{out1} = 456V$ and $V_{out2} = 433V$.

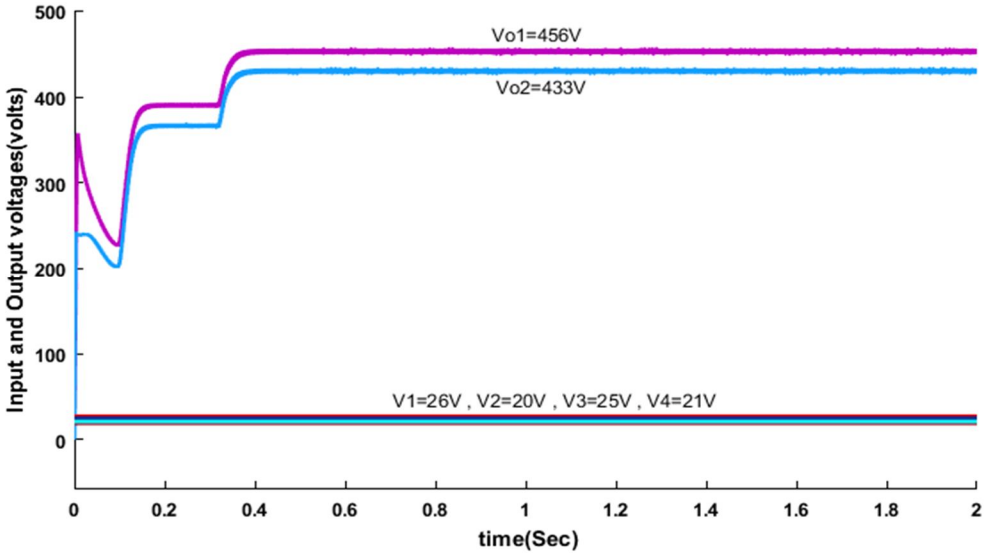


Figure.14.Input and Output Voltage waveforms of a four-input two-output Boost converter with PI controller

## IX. CONCLUSION

In this paper Closed loop control of a new MIMO high step-up DC-DC converter is proposed. Also, in order to increase each output voltage, diode-capacitor voltage multiplier (VM) stages are utilized in the proposed converter. A power sharing process can be applied among the input sources and output loads to control the contribution of each input sources in supplying the output loads. Typically such converter helps in integrating many sources which directly generate DC power. For each modes of operation, transfer function matrices are obtained separately and compensators for closed loop control of the converter is designed. It can be seen that, under fault conditions or change in input voltage cannot change the output voltage. Finally the converter operation, theoretical calculations and simulation results are verified. The efficiency is 95.96%

## REFERENCES

[1] Faraz Ahmad, Aziz Ahmad Haider, Hassan Naveed, Atay Mustafa, Irshad Ahmad"Multiple Input Multiple output DC-DC Converter," 2018 5th International Multi-Topic ICT Conference (IMTIC), IEEE.
[2] B. Dobbs and P. Chapman, "A multiple-input DC-DC converter topology," IEEE Power Electronics Letters, vol. 99, no. 1, pp. 6–9, mar 2003.
[3] Y. Tong, Z. Shan, J. Jatskevich, and A. Davoudi, "A nonisolated multiple-input multiple-output dc-dc converter for dc distribution of future energy efficient homes," in Ind. Electron. Society, IECON 2014 40th Annual Conference of the IEEE, 2014, pp. 4126-4132: IEEE.
[4] H. Keyhani and H. A. Toliyat, "A ZVS single-inductor multi-input multi-output DC-DC converter with the step up/down capability," in Energy Conversion Congress and Exposition (ECCE), 2013 IEEE, 2013, pp. 5546-5552: IEEE.
[5] H. Behjati and A. Davoudi, "Single-stage multi-port DC–DC converter topology," IETPower Electron., vol. 6, no. 2, pp. 392-403, 2013.

[6] H. Behjati and A. Davoudi, "A multiple-input multiple-output DC–DC converter," IEEE Trans. Ind. Appl., vol. 49, no. 3, pp. 1464-1479, 2013.
[7] M. Jafari, G. Hunter, and J. G. Zhu, "A new topology of multi-input multi-output Buck-Boost DC-DC Converter for microgrid applications," in Power and Energy (PECon), 2012 IEEE Int. Conf., 2012, pp. 286291: IEEE.
[8] A. Nahavandi, M. T. Hagh, M. B. B. Sharifian, and S. Danyali, "A nonisolated multiinput multioutput DC–DC boost converter for electric vehicle applications," IEEE Trans. Power Electron., vol. 30, no. 4, pp. 1818-1835, 2015.
[9] M. R. Banaei, H. Ardi, R. Alizadeh, and A. Farakhor, "Non-isolated multi-input–single-output DC/DC converter for photovoltaic power generation systems," IET Power Electron., vol. 7, no. 11, pp. 2806-2816, 2014.
[10] N. kumar Reddi, M. Ramteke, H. Suryawanshi, K. Koteswararao, and S. Gawande, "An Isolated Multi-Input ZCS DC-DC Front-End-Converter Based Multilevel Inverter for the Integration of Renewable Energy Sources," IEEE Trans. Ind. Appl., 2017.
[11] S. Dusmez, X. Li, and B. Akin, "A new multiinput three-level DC/DC converter," IEEE Trans. Power Electron., vol. 31, no. 2, pp. 1230-1240, 2016.
[12] E. Babaei and O. Abbasi, "Structure for multi-input multi-output dc–dc boost converter," IET Power Electron., vol. 9, no. 1, pp. 9-19, 2016.
[13] S. Danyali, S. H. Hosseini, and G. B. Gharehpetian, "New extendable single-stage multi-input DC–DC/AC boost converter," IEEE Transactions on power electronics, vol. 29, no. 2, pp. 775-788, 2014.

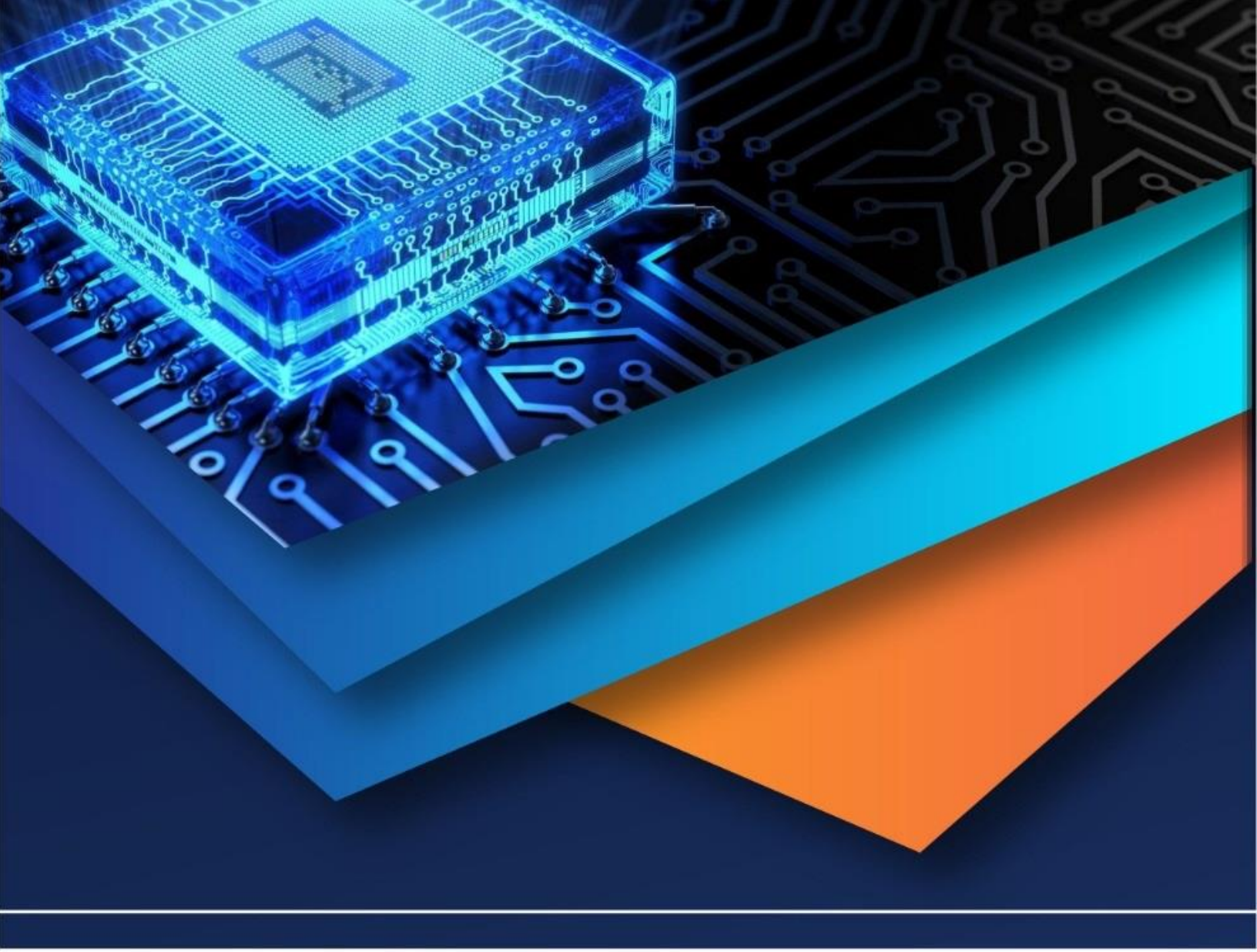

10.22214/IJRASET

45.98

IMPACT FACTOR: 7.129

IMPACT FACTOR: 7.429

# INTERNATIONAL JOURNAL FOR RESEARCH

IN APPLIED SCIENCE & ENGINEERING TECHNOLOGY